



Published in final edited form as:

Neuroimage Rep. 2025 March ; 5(1): . doi:10.1016/j.ynirp.2025.100234.

## Cholinergic neurotransmission in the anterior cingulate cortex is associated with cognitive performance in healthy older adults: Baseline characteristics of the Improving Neurological Health in Aging via Neuroplasticity-based Computerized Exercise (INHANCE) trial

Ana de Figueiredo Pelegrino<sup>a,\*</sup>, Mouna Attarha<sup>b</sup>, Paule-Joanne Toussaint<sup>a</sup>, Lydia Ouellet<sup>a</sup>, Sarah-Jane Grant<sup>b</sup>, Thomas Van Vleet<sup>b</sup>, Etienne de Villers-Sidani<sup>a</sup>

<sup>a</sup>McGill University, Montreal Neurological Institute and Hospital, 3801 University Street, Montréal, Quebec, H3A 2B4, Canada

<sup>b</sup>Posit Science Corporation, 160 Pine St Suite 200, San Francisco, CA, 94111, United States

### Abstract

Aging is associated with dysfunction in the cholinergic system, including degeneration of basal forebrain cholinergic terminals that innervate the cortex, which directly contributes to age- and disease-related cognitive decline. In this study, we used [18F]fluoroethoxybenzovesamicol ([18F]FEOBV) positron emission tomography (PET) imaging to assess the effect of age on cholinergic terminal integrity in predefined regions of interest and its relationship to cognitive performance in healthy older adults who underwent neuropsychological assessment and FEOBV PET brain imaging. Our results showed age-related reductions in FEOBV binding, particularly in the anterior cingulate cortex-the primary region of interest-as well as in the striatum, posterior cingulate cortex, and primary auditory cortex. Notably, FEOBV binding in the anterior cingulate cortex was positively correlated with cognitive performance on the NIH EXAMINER Executive Composite Score. These findings suggest that [18F] FEOBV PET imaging can be used as a reliable biomarker to assess cholinergic changes in the human brain and indicate that preserving the cholinergic integrity of the basal forebrain may help maintain cognitive function and protect against age-related cognitive decline.

This is an open access article under the CC BY-NC-ND license (<http://creativecommons.org/licenses/by-nc-nd/4.0/>).

\*Corresponding author. ana.pelegrino@mail.mcgill.ca (A. de Figueiredo Pelegrino).

CRediT authorship contribution statement

**Ana de Figueiredo Pelegrino:** Writing – review & editing, Writing – original draft, Visualization, Methodology, Formal analysis, Data curation. **Mouna Attarha:** Writing – review & editing, Visualization, Supervision, Software, Resources, Methodology, Funding acquisition, Formal analysis, Data curation, Conceptualization. **Paule-Joanne Toussaint:** Writing – review & editing, Project administration, Methodology, Formal analysis. **Lydia Ouellet:** Project administration, Investigation. **Sarah-Jane Grant:** Validation, Software, Project administration, Investigation, Data curation. **Thomas Van Vleet:** Writing – review & editing, Supervision, Resources, Methodology, Funding acquisition, Conceptualization. **Etienne de Villers-Sidani:** Writing – review & editing, Supervision, Resources, Methodology, Formal analysis, Conceptualization.

Declaration of competing interest

The authors declare that they have no known competing financial interests or personal relationships that could have appeared to influence the work reported in this paper.

## Keywords

Aging; Cognitive decline; Cholinergic system; [18F]FEOBV PET

---

## 1. Introduction

The process of natural aging is associated with moderate structural and functional degeneration in the basal forebrain cholinergic neurotransmitter system (Altavista et al., 1990; Gasiorowska et al., 2021). These age-related changes in cholinergic neurotransmission are thought to contribute to the decline in cognitive functions that are commonly observed with aging (Ballinger et al., 2016; Everitt and Robbins, 1997; McGeer et al., 1984; Schliebs and Arendt, 2011). Indeed, cholinergic projections from the basal forebrain play a crucial role in cognitive performance due to their involvement in high-order cognitive functions such as attention, learning and memory, and executive function (Ballinger et al., 2016; Schliebs and Arendt, 2011; Hasselmo and Sarter, 2011). For example, enhancing cholinergic signaling has been demonstrated to enhance attention and memory performance in individuals with naturally lower cognitive performance (Knott et al., 2015; Niemegeers et al., 2014). Consequently, cholinergic signaling has been identified as a potential key factor in age-related cognitive diseases, such as mild cognitive impairment (MCI) and Alzheimer's disease (Ballinger et al., 2016; Hampel et al., 2019). For instance, degeneration of basal forebrain cholinergic neurons can occur years before the onset of cognitive symptoms and may predict both cortical pathology and memory impairment (Fernández-Cabello et al., 2020; Schmitz and Nathan Spreng, 2016). Understanding age-related changes in the cholinergic system is crucial for elucidating the contribution of aging to cognitive decline and for identifying those who are at risk for age-related cognitive diseases marked by cholinergic degeneration.

[18F]Fluoroethoxybenzovesamicol ([18F]FEOBV) is a reliable positron emission tomography (PET) tracer for the direct assessment of cerebral cholinergic neurotransmission in vivo. This high-affinity tracer binds to the vesicular acetylcholine transporter (VACHT), thereby enabling precise measurement of presynaptic cholinergic terminal density (Petrou et al., 2014). The binding pattern of [18F]FEOBV across cortical and subcortical areas reflects the unique organization of the cholinergic system, with decreases in binding indicating regions that show reduced cholinergic terminal densities due to natural aging (Albin et al., 2018) and age-related cognitive diseases (Aghourian et al., 2021; van der Zee et al., 2021; Xia et al., 2022). For example, substantial declines in FEOBV binding have been documented across the entire cortex in individuals with Alzheimer's disease, with higher binding levels associated with superior performance on global cognitive assessments (Aghourian et al., 2017; Schmitz et al., 2018). Similarly, reductions in cortical FEOBV binding have been observed in individuals with MCI, with binding levels positively correlating with executive function and attention in a cohort that included MCI patients and cognitively intact older adults (Xia et al., 2022). In natural aging, a recent study found reduced FEOBV binding in the anterior cingulate cortex of healthy older compared to younger subjects (Albin et al., 2018). The anterior cingulate cortex plays a key role in attention, memory, and executive function (Martinelli et al., 2013; Pardo et al., 2020; Posner

and Rothbart, 1998). Notably, greater anterior cingulate thickness has been associated with successful cognitive aging (Pezzoli et al., 2024), whereas atrophy in this region has been linked to impaired cognitive function (Tan et al., 2013).

This paper presents the baseline characteristics of the intent-to-treat population in the Improving Neurological Health in Aging via Neuroplasticity-based Computerized Exercise (INHANCE) trial – a Phase IIb double-blind randomized controlled study targeting community-dwelling healthy older adults aged 65 and above. Participants were randomized to receive either 35 h of a computerized speed and attention brain training intervention (BrainHQ) or an active control involving computerized games over a 10-week period. In the largest [18F]FEOBV PET study in neurocognitively intact older adults to date, we used volume-of-interest analysis, focusing on a priori-selected regions of interest, to evaluate: (1) the impact of age on cholinergic neurotransmission, and (2) the relationship between cholinergic neurotransmission and cognitive performance. Considering previous findings, we anticipated age-related reductions in FEOBV binding in the primary region of interest, the anterior cingulate cortex. We also anticipated that higher FEOBV binding in the anterior cingulate cortex would be associated with better cognitive performance.

## 2. Methods

### 2.1. Study design

The INHANCE trial is a double-blind, parallel design, active-controlled, randomized clinical trial to evaluate the superiority of 35 h over 10 weeks (~30 min per session, 7 sessions per week, for a total of 70 sessions) of computerized speed and attention brain training intervention (BrainHQ by Posit Science) compared to an active control group of computer games (bricks breaker and solitaire) in healthy older adults.

**2.1.1. Randomization**—Detailed information regarding the randomization procedures and intervention is available in the published protocol (Attarha et al., 2024). Briefly, participants were randomized to either computerized speeded brain training or to a non-speeded active control. Participants were blinded to group assignment, and the research team performing the assessments did not have access to participants' group assignments. The groups were balanced based on the distribution of acetylcholine levels and the NIH EXAMINER composite score (flanker, set-shifting and antisaccade subtests) (Kramer et al., 2014). Previous research has shown that FEOBV binding in the anterior cingulate decreases significantly with age, whereas binding in the occipital cortex does not (Albin et al., 2018). The acetylcholine score was defined as the ratio of anterior cingulate to occipital cortex to account for inter-individual differences in baseline binding.

Study staff supporting participants remained unblinded, while blinded staff conducted assessments, scoring, follow-ups, and baseline data analyses.

### 2.2. Participants

The INHANCE trial took place at McGill University, Canada, where the FEOBV radiotracer was both synthesized and administered. Below, we outline the methodological details

pertinent to this paper. A comprehensive description of the training programs, measures, and data analyses can be found in the study protocol (Attarha et al., 2024).

Inclusion criteria comprised individuals aged 65 or older, proficient in English or French, cognitively intact with a Montreal Cognitive Assessment (MoCA) score of  $\geq 23$  Carson et al., 2018, a cut-off that optimizes sensitivity and specificity, and capable of fulfilling study requirements. Exclusion criteria encompassed neurocognitive disorders, suicidal ideation, major depression scoring  $>10$  on the Geriatric Depression Scale – Short Form (GDS-SF), prior experience with BrainHQ within the past 5 years, concurrent clinical trial participation, pregnancy, substance abuse, neuroimaging contraindications, or medical conditions hindering study engagement.

The study protocol was developed in accordance with the Declaration of Helsinki guidelines and was approved by WIRB (IRB00000533) and REB of McGill University Health Centre (2020–6474). The radio-ligand FEOBV was approved by Health Canada (Control # 252085). All participants provided written, informed consent.

### 2.3. Imaging acquisition

All participants underwent a structural T1-weighted MRI scan (3T Siemens Prisma) using the 3D magnetization-prepared rapid gradient echo (MPRAGE) sequence, and a [18F]FEOBV-PET scan using the Siemens High-Resolution Research Tomograph (HRRT) at the McConnell Brain Imaging Centre of the Montreal Neurological Institute-Hospital. Concurrent T1-weighted MPRAGE images were acquired with the related acquisition parameters being echo time/repetition time = 2.98 ms/2300 ms, inversion time = 900 s, flip angle  $9^\circ$ , 1 mm isotropic resolution, and image dimensions  $192 \times 256 \times 256$ .

The [18F]FEOBV precursor (ABX Advanced Biochemical Compounds, GmbH, Germany) was synthesized on the same day as participant testing at the cyclotron facility. Radiochemical purity was ensured using high-performance liquid chromatography. Mass dosages did not exceed the proposed limits of 0.0175 mcg/kg (Petrou et al., 2014). Participants received a slow bolus intravenous injection of [18F]FEOBV with radioactivity doses ranging from 350 to 400 MBq. PET data acquisition started 180 min after injection, for a duration of 30 min, divided into 6 frames of 5 min each. All PET imaging sessions were supervised by a qualified nuclear medicine physician.

Participants reported a total of 53 adverse events of which 4 (7.5%) were related to the administration of [18F]FEOBV tracer. Of those 4 reports, one participant reported 2 events (mild dry mouth, mild strange sensations in the mouth) and a second participant reported 2 events (moderate nausea, moderate vomiting). Both recovered without treatment. No serious adverse events were reported.

### 2.4. PET and MRI data processing

A transmission scan of 5 min was conducted with a rotating point source of [137Cs] for the HRRT PET images in order to perform attenuation correction. Images were reconstructed using an ordinary Poisson-ordered subset expectation maximization (OP-OSEM) algorithm correcting for scattering, random chance, attenuation, decay, and dead time. Motion

correction algorithms were applied. The raw PET data were time-averaged over their 6 frames to create a static PET image, and reconstructed using resolution recovery, 10 iterations and 16 subsets, on a  $256 \times 256 \times 207$  matrix, resulting in a voxel size of 1.22 mm<sup>3</sup> and a spatial resolution of 2.3 mm full-width at half-maximum (FWHM). No post-reconstruction smoothing filter or zoom was applied.

SPM12 (<http://fil.ion.ucl.ac.uk/spm/>) for MATLAB was used for the following preprocessing steps. The MRIs were aligned to the MNI 152 asymmetrical template (MNI152 ONLine, 2009 cAsym template) for segmentation (into native and ‘Dartel-imported’ gray matter, white matter and cerebrospinal fluid) and bias correction. The static PET images were aligned with the subject’s corresponding MRI. Müller-Gärtner partial volume correction was applied to the PET data using the PETPVE toolbox to remove the partial volume effect. The spatial normalization of the MRIs to the MNI152 template was achieved using the high-dimensional registration algorithm DARTEL with identical transformations being applied to the PET images. To reduce noise, a Gaussian smoothing kernel with a FWHM of 6 mm was applied to the PET images. All preprocessing steps were conducted with appropriate quality control checks, ensuring data integrity and consistency throughout the process.

For all spatially normalized FEOBV PET images, the mean standard uptake value ratios (SUVR) were computed in pre-selected regions of interest (ROI) using a white matter mask as a reference region to normalize the PET images (Nejad-Davarani et al., 2019). Anatomical MNI-space Hammers atlas (Hammers et al., 2003) was applied to the PET images to quantify regional differences in FEOBV binding in the anterior cingulate cortex (Matched MNI-space region: anterior cingulate), striatum (Matched MNI-space region: putamen and caudate), posterior cingulate cortex (Matched MNI-space region: posterior cingulate), primary sensorimotor cortex (Matched MNI-space region: precentral gyrus and postcentral gyrus), global cortex (frontal, temporal, occipital and parietal cortices), hippocampus (Matched MNI-space region: hippocampus), and parahippocampal gyrus (Matched MNI-space region: parahippocampal gyrus). The [Jülich Brain cytoarchitectonic atlas](#) was used to quantify the binding in the primary auditory cortex (Matched MNI-space region: TE1.0, TE1.1, TE1.2).

## 2.5. Outcome measures

The endpoints relevant to the current paper include (1) baseline FEOBV binding in the a priori selected primary ROI (anterior cingulate cortex) and pre-specified exploratory ROIs (posterior cingulate cortex, primary auditory cortex, primary sensorimotor cortex, parietal lobe, frontal lobe, occipital lobe, temporal lobe, global cortex, hippocampus, parahippocampal gyrus, putamen, caudate, striatum), and (2) baseline cognitive performance using the executive composite z-score from the NIH EXAMINER battery (flanker, set-shifting and antisaccade subtests) (Kramer et al., 2014).

The selection of ROIs was guided by two complementary rationales: (1) previous findings from Albin et al. (2018) and Kanel et al. (2022) showing reduced FEOBV binding in specific brain regions, and (2) the hypothesized effects of the attention-focused brain

training on cholinergic neurotransmission in brain regions supporting attention and executive function.

## 2.6. Statistical analysis

The distributions of the FEOBV SUVR for each ROI were tested for normality using the Shapiro-Wilk Test. To evaluate the association between FEOBV binding and age, we conducted Pearson correlations between baseline FEOBV SUVRs and age in years reported by the intent-to-treat (ITT) in the primary region of interest (i.e. anterior cingulate cortex) and exploratory ROIs. To evaluate the association between FEOBV binding and cognitive performance, we conducted Pearson correlations between baseline FEOBV SUVR in the primary region of interest (i.e. anterior cingulate cortex) and exploratory ROIs, and the baseline cognitive composite z-score from the NIH EXAMINER battery.

No correction for multiple comparisons is made for exploratory analyses as specified in the published protocol (Attarha et al., 2024). All trending relationships ( $p < 0.10$ ) are reported.

## 3. Results

### 3.1. Participants

The flowchart of participants is depicted in Fig. 1. Out of 113 individuals who were consented and screened, 20 were excluded for not meeting the criteria. Additionally, one participant was withdrawn by the site Principal Investigator before starting the assigned training program due to incidental findings on baseline imaging that precluded participation in the study. Thus, 92 participants completed the baseline neuropsychological assessments and neuroimaging sessions.

### 3.2. Baseline characteristics of the intent-to-treat population

Demographic and neuropsychological characteristics for this study cohort ( $N = 92$ ) are summarized in Table 1.

### 3.3. Distribution of [18F]FEOBV PET signal

Brain FEOBV binding exhibited non-uniform distribution across various brain regions. The highest tracer binding was present in the striatum (putamen > caudate), followed by the hippocampus and cortical areas. The general distribution of [18F]FEOBV binding is described in Table 2 and Fig. 2.

### 3.4. Association of FEOBV binding with age and MoCA for the intent-to-treat population

Baseline FEOBV SUVR was negatively associated with age in the anterior cingulate cortex, with lower uptake observed in older adults ( $r = -0.29$ ,  $p = 0.005$ , Fig. 3).

To further investigate predictors of FEOBV binding changes in the anterior cingulate cortex, a multiple linear regression analysis was conducted, including age, sex, and education as predictors. The overall model accounted for 8.6% of the variance in FEOBV binding ( $F(3, 87) = 2.73$ ,  $p = 0.049$ ,  $R = 0.29$ ,  $R^2 = 0.086$ ). Among the predictors, only age was a significant predictor of changes in FEOBV binding in the anterior cingulate cortex. The



unstandardized coefficient indicates that for each additional year of age, FEOBV binding in the anterior cingulate cortex decreases by 0.011 units ( $B = -0.011$ ,  $\text{Beta} = -0.28$ ,  $t = -2.81$ ,  $p = 0.006$ ). With a baseline SUVR of 1.90, this corresponds to an estimated annual decrease of 0.58%, and a projected cumulative decrease of 5.8% over a decade, assuming a linear relationship. In contrast, sex ( $B = 0.002$ ,  $\text{Beta} = 0.004$ ,  $t = 0.042$ ,  $p = 0.96$ ) and education ( $B = 0.001$ ,  $\text{Beta} = 0.044$ ,  $t = 0.42$ ,  $p = 0.67$ ) did not significantly affect FEOBV binding.

Baseline FEOBV SUVR values exhibited a significant negative association with age in exploratory regions of interest (ROIs). Specifically, negative correlations were observed in the striatum ( $r = -0.26$ ,  $p = 0.01$ ); putamen ( $r = -0.27$ ,  $p = 0.01$ ) and caudate ( $r = -0.21$ ,  $p = 0.05$ ), primary auditory cortex ( $r = -0.28$ ,  $p = 0.008$ ) and posterior cingulate cortex ( $r = -0.20$ ,  $p = 0.05$ ). See Table 2. The unstandardized coefficients indicate that for each additional year of age, FEOBV binding decreases by 0.04 units in the striatum ( $B = -0.04$ ,  $\text{Beta} = -0.24$ ,  $t = -2.43$ ,  $p = 0.01$ ), 0.017 units in the primary auditory cortex ( $B = -0.017$ ,  $\text{Beta} = -0.26$ ,  $t = -2.63$ ,  $p = 0.01$ ), and 0.009 units in the posterior cingulate cortex ( $B = -0.009$ ,  $\text{Beta} = -0.22$ ,  $t = -2.16$ ,  $p = 0.04$ ). Given baseline SUVR values of 6.09 in the striatum, 2.01 in the primary auditory cortex, and 1.94 in the posterior cingulate cortex, these reductions suggest annual decreases of 0.66%, 0.85%, and 0.46%, respectively, which, if sustained, could correspond to projected cumulative reductions of 6.7%, 8.46%, and 4.64% over a decade. No significant associations were found in the remaining ROIs.

No significant associations were found between FEOBV binding and MoCA. See Table 2.

### 3.5. Association between FEOBV binding and cognition for the intent-to-treat population

Baseline FEOBV SUVR in the anterior cingulate cortex exhibited a positive correlation with baseline NIH EXAMINER executive composite z-score ( $r = 0.23$ ,  $p = 0.027$ , Fig. 4). This indicates that reduced FEOBV binding in the anterior cingulate is associated with reduced cognitive performance. No significant associations were found across other exploratory ROIs. See Table 2.

## 4. Discussion

In this study, we used [18F]FEOBV PET imaging to examine cholinergic nerve terminal distribution and its relationship with cognition in a large cohort of 92 neurocognitively intact older adults. We observed age-related reductions in FEOBV binding in the primary region of interest, the anterior cingulate cortex. Given the extensive projections of basal forebrain cholinergic neurons throughout the cortex and subcortical regions, as well as previous findings of age-related declines in binding across these areas, we conducted an exploratory analysis in additional ROIs. Significant age-related decreases in FEOBV binding were observed in the striatum (putamen and caudate), primary auditory cortex and posterior cingulate cortex. Additionally, FEOBV binding in the anterior cingulate cortex positively correlated with cognitive performance on the NIH EXAMINER executive composite score.

Current evidence suggests that [18F]FEOBV reliably assesses changes in the integrity of the brain's acetylcholine system (Petrone et al., 2014; Aghourian et al., 2021; van der Zee et al., 2021; Okkels et al., 2023), with its binding distribution reflecting the known anatomical

distribution of cholinergic terminals (Mesulam, 2004, 2013). In our study, the distribution of the [18F]FEOBV tracer was highest in the striatum, with greater binding observed in the putamen compared to the caudate, followed by the hippocampus and cortical regions. Overall, this heterogeneous cholinergic distribution is similar to previous histological post-mortem studies of brain cholinergic innervation in humans (Okkels et al., 2023; Mesulam, 2004), as well as observed in rats (Parent et al., 2012; Rosa-Neto, 2007) and non-human primates (Soucy et al., 2010).

We confirmed that aging is associated with reduced acetylcholine neurotransmission in the anterior cingulate cortex and striatum of healthy older adults, as evidenced by decreased FEOBV binding with age. Specifically, FEOBV binding declined by approximately 5.8% per decade in the anterior cingulate cortex and 6.7% in the striatum. Similarly, Albin et al. (2018) recently used [18F]FEOBV PET imaging to investigate the topography of brain cholinergic innervation in 29 healthy subjects, with a mean age of 47 years (range 20–81 years). Using region-based analysis, they reported age-related reductions in FEOBV binding, including approximately a 4% decrease per decade in the striatum and a 2.5% decrease per decade in both the primary sensorimotor cortex and anterior cingulate cortex (Albin et al., 2018). These results were later confirmed by a whole brain voxel-based analysis study in a larger sample with 42 healthy subjects (mean age 50 years, range 20–80 years) (Kanel et al., 2022). Unexpectedly, Okkels et al. (2023) found similar levels of regional FEOBV binding in a cohort of 20 neurocognitively intact older adults (mean age 74 years, range 64–86 years) (Okkels et al., 2023). These contrasting results may stem from differences in age ranges, sample size limitations, and the type of analysis used (region-vs. voxel-based). While a voxel-wise approach offers a more detailed view of the whole brain, it may have greater variability in identifying region-specific effects in smaller samples with restricted age ranges.

Overall, our findings align with the existing literature demonstrating region-specific decreases in FEOBV binding that may reflect age-related changes in key basal forebrain cholinergic groups, including reduced cholinergic terminals in the nucleus basalis of Meynert (Ch4), which innervates the entire cerebral cortex (Mesulam, 2004). Interestingly, this process does not appear to be uniform. Significant decreases in FEOBV binding were observed in cortical regions such as the anterior cingulate, posterior cingulate, and primary auditory cortices, whereas other regions, like the primary sensorimotor cortex, showed no age-related changes. Similarly, Albin et al. (2018) and Kanel et al. (2022) reported non-uniform patterns of age-related reductions across the cortex. Furthermore, reduced FEOBV binding in the striatum suggests reductions in striatal cholinergic interneuron terminals, which serve as the primary source of cholinergic input to this region (Lim et al., 2014). Surprisingly, we found no significant age-related reductions in FEOBV binding in the parahippocampal gyrus or hippocampus, contrasting with findings by Kanel et al. (2022), who reported age-related reductions in these regions in a cohort of 42 cognitively normal older adults (mean age 50 years, range 20–80 years). Age-related reductions in FEOBV binding in the hippocampus were also observed in aged rats (Parent et al., 2012). This difference suggests that cholinergic innervation from the medial septal nucleus (Ch1) and the vertical limb of the diagonal band (Ch2) (Mesulam, 2004) to the hippocampus may be preserved in our cohort of healthy older adults. Interestingly, in patients with Alzheimer's



disease, Aghourian et al. (2021) reported no significant associations between FEOBV binding in the hippocampus and Ch1-2 volume, consistent with literature indicating that this region remains relatively unaffected by cholinergic denervation in the disease (Aghourian et al., 2021). In summary, because natural aging affects cholinergic systems heterogeneously, some regions, such as Ch1-2, may be potentially more resistant to age-related changes compared to others, such as Ch4.

Furthermore, we investigated the relationship between FEOBV binding and NIH executive composite score. Notably, we observed a positive correlation between FEOBV binding in the anterior cingulate cortex and the NIH executive composite score in healthy older adults. To our knowledge, this is the first study to observe a positive association between FEOBV binding in the anterior cingulate cortex and cognitive performance in a large sample of neurocognitively intact older adults. Xia et al. reported positive correlations between global cortical FEOBV SUVR and cognitive composite scores for executive function ( $r = 0.70$ ) and attention ( $r = 0.60$ ) in a cohort of 18 individuals with MCI and cognitively intact older adults. For executive function, correlations were widespread across cortical and subcortical regions, while for attention, significant clusters were mainly in the anterior cingulate gyrus (Xia et al., 2022). Moreover, in a large sample of cognitively unimpaired Parkinson's disease patients, positive associations were observed between global cortical FEOBV binding and cognitive performance across memory, executive functioning, and attention domains (van der Zee et al., 2021). Additionally, neurodegeneration in the nucleus basalis of Meynert preceded and predicted cortical degeneration and memory impairment in patients with Alzheimer's disease (Fernández-Cabello et al., 2020).

The mechanisms underlying age-related impairments in basal forebrain cholinergic neurotransmission are not fully understood. Possible biological factors may contribute to this decline. One key factor is the sensitivity of cholinergic neurons to disruptions in nerve growth factor signaling, which is crucial for their protection and maintenance. Such disruptions can lead to cellular atrophy and alterations in gene expression (Sofroniew et al., 2001). Additionally, basal forebrain cholinergic neurons, characterized by their extensive axonal projections, are particularly susceptible to metabolic disturbances. The substantial energy requirements needed to maintain these widespread connections throughout life may underlie the vulnerability of the basal forebrain cholinergic system to neurodegenerative diseases (Ballinger et al., 2016). Given the critical role of these cholinergic neurons in important cognitive processes, the degenerative changes observed in cortical cholinergic terminals during normal aging likely contribute significantly to age-related cognitive decline. Indeed, augmenting acetylcholine levels through acetylcholinesterase inhibitors, has demonstrated cognitive enhancements in individuals with MCI and Alzheimer's disease (Rockwood, 2004; Moreira et al., 2022), underscoring the significance of acetylcholine in preserving the integrity of the brain and cognitive function (Hempel et al., 2018). These findings collectively highlight the pivotal role of the cholinergic system in maintaining cognitive health and its potential as a target for interventions to mitigate age-related cognitive decline.

Limitations of this study first include the use of a limited volume-of-interest analysis based on an a priori selection of regions with relatively age-related reductions in FEOBV binding

reported in previous studies. A more spatially unbiased analysis would facilitate a more comprehensive assessment of the effects of aging on cholinergic neurotransmission. Second, we did not assess neurodegenerative biomarkers like amyloid-beta and tau, which could potentially confound our findings since tauopathy in the nucleus basalis of Meynert can lead to degeneration of cholinergic axons (Mesulam, 2013). While Xia et al. (2022) reported no significant differences in global cortical FEOBV binding between amyloid-beta-positive and -negative cognitively intact older adults, the small cohort size limits the conclusiveness of these results. Therefore, further studies with larger sample sizes are necessary to robustly assess the impact of neuropathologies on FEOBV binding and cognitive performance in healthy older adults. Third, while a MoCA cutoff of 23/30 balances sensitivity and specificity better than 26/30,<sup>27</sup> it may not fully exclude individuals with MCI. This cutoff was selected to account for age-related variability in scores, ensuring a broader representation of healthy aging and avoiding bias toward the highest-functioning individuals. Such approach aligns with the primary goal of the INHANCE trial, which is to assess the effects of speed-based cognitive training on cholinergic neurotransmission and cognition. Importantly, no significant correlations were found between FEOBV binding and MoCA scores. Lastly, we did not exclude participants with vascular health conditions, such as diabetes and hypertension. Given the widespread prevalence of these metabolic conditions in older adults aged 65 years and older and the lack of specific diagnostic labels for hypertension- or diabetes-associated cognitive impairment, we did not include these as exclusion criteria in the INHANCE trial to maximize the generalizability of the intervention outcome results. We further note no a priori reason to expect that individuals with vascular risk factors would not benefit from a computerized brain training intervention; in fact, pre/post cognitive gains are observed in individuals with diabetes and a history of stroke (Natovich et al., 2020; Cuevas et al., 2020; Chen et al., 2015).

## 5. Conclusion

In conclusion, we demonstrate that key cholinergic terminals, including those originating from the nucleus basalis of Meynert and striatal cholinergic interneurons, are particularly vulnerable to the effects of natural aging, with age-related changes in FEOBV distribution in the anterior cingulate cortex potentially playing a crucial role in cognitive decline. Our study adds to the literature by showing that [18F] FEOBV PET imaging is an effective marker for assessing changes in cholinergic neurotransmission, suggesting that maintaining an intact basal forebrain cholinergic system may provide cognitive resilience and protect against both age- and disease-related cognitive decline.

## Acknowledgements

We would like to thank the members of McGill's Clinical Research and PET Imaging Units, and the software engineers and quality assurance team at Posit Science.

## Funding sources

Research reported in this publication was supported by the National Institute on Aging of the National Institutes of Health under Award Numbers R44AG039965 and 3R44AG039965-06S1 awarded to MA and TVV. The funders had no role in design and conduct of the study; collection, management, analysis, and interpretation of the data; preparation, review, or approval of the manuscript; and decision to submit the manuscript for publication. This

content is solely the responsibility of the authors and does not necessarily represent the official views of the National Institutes of Health.

## Data availability

Data available: Yes.

Data types: Deidentified participant data (imaging, cognitive, behavioral)

When available: Two years after trial completion (on May 31, 2026), the INHANCE dataset will be made available to verified academic and industry researchers. Investigators can conduct both confirmatory and exploratory analyses using LORIS, a freely accessible, open-source data archive with provenance-sharing features. Access the dataset here: <https://inhance.loris.ca/>

## References

- Aghourian M, Legault-Denis C, Soucy JP, et al. , 2017. Quantification of brain cholinergic denervation in Alzheimer's disease using PET imaging with [18F]-FEOBV. *Mol. Psychiatr* 22 (11), 1531–1538. 10.1038/mp.2017.183.
- Aghourian M, Aumont É, Grothe MJ, Soucy JP, Rosa-Neto P, Bedard MA, 2021. FEOBV-PET to quantify cortical cholinergic denervation in AD: relationship to basal forebrain volumetry. *J. Neuro. Off. J. Am. Soc. Neuroimaging* 31 (6), 1077–1081. 10.1111/jon.12921.
- Albin RL, Bohnen NI, Muller ML, et al. , 2018. Regional vesicular acetylcholine transporter distribution in human brain: a [18F]fluoroethoxybenzovesamicol positron emission tomography study. *J. Comp. Neurol* 526 (17), 2884–2897. 10.1002/cne.24541. [PubMed: 30255936]
- Altavista MC, Rossi P, Bentivoglio AR, Crociani P, Albanese A, 1990. Aging is associated with a diffuse impairment of forebrain cholinergic neurons. *Brain Res.* 508 (1), 51–59. 10.1016/0006-8993(90)91116-x. [PubMed: 2337791]
- Attarha M, de Figueiredo Pelegriño AC, Toussaint PJ, Grant SJ, Van Vleet T, de Villers-Sidani E, 2024. Improving neurological health in aging via neuroplasticity-based computerized Exercise: protocol for a randomized controlled trial. *JMIR Res. Protoc* 13, e59705. 10.2196/59705. [PubMed: 39116435]
- Ballinger EC, Ananth M, Talmage DA, Role LW, 2016. Basal forebrain cholinergic circuits and signaling in cognition and cognitive decline. *Neuron* 91 (6), 1199–1218. 10.1016/j.neuron.2016.09.006. [PubMed: 27657448]
- Carson N, Leach L, Murphy KJ, 2018. A re-examination of Montreal Cognitive Assessment (MoCA) cutoff scores. *Int. J. Geriatr. Psychiatr* 33 (2), 379–388. 10.1002/gps.4756.
- Chen CX, Mao RH, Li SX, Zhao YN, Zhang M, 2015. Effect of visual training on cognitive function in stroke patients. *Int. J. Nurs. Sci* 2 (4), 329–333. 10.1016/j.ijnss.2015.11.002.
- Cuevas HE, Stuijbergen AK, Brown SA, 2020. Targeting cognitive function: development of a cognitive training intervention for diabetes. *Int. J. Nurs. Pract* 26 (5), e12825. 10.1111/ijn.12825. [PubMed: 32030848]
- Everitt BJ, Robbins TW, 1997. Central cholinergic systems and cognition. *Annu. Rev. Psychol* 48, 649–684. 10.1146/annurev.psych.48.1.649. [PubMed: 9046571]
- Fernández-Cabello S, Kronbichler M, Van Dijk KRA, et al. , 2020. Basal forebrain volume reliably predicts the cortical spread of Alzheimer's degeneration. *Brain* 143 (3), 993–1009. 10.1093/brain/awaa012. [PubMed: 32203580]
- Gasiorowska A, Wydrych M, Drapich P, et al. , 2021. The biology and pathobiology of glutamatergic, cholinergic, and dopaminergic signaling in the aging brain. *Front. Aging Neurosci* 13, 654931. 10.3389/fnagi.2021.654931. [PubMed: 34326765]

- Hammers A, Allom R, Koepp MJ, et al. , 2003. Three-dimensional maximum probability atlas of the human brain, with particular reference to the temporal lobe. *Hum. Brain Mapp* 19 (4), 224–247. 10.1002/hbm.10123. [PubMed: 12874777]
- Hempel H, Mesulam MM, Cuello AC, et al. , 2018. The cholinergic system in the pathophysiology and treatment of Alzheimer's disease. *Brain J. Neurol* 141 (7), 1917–1933. 10.1093/brain/awy132.
- Hempel H, Mesulam MM, Cuello AC, et al. , 2019. Revisiting the cholinergic hypothesis in Alzheimer's disease: emerging evidence from translational and clinical research. *J. Prev. Alzheimers Dis* 6 (1), 2–15. 10.14283/jpad.2018.43. [PubMed: 30569080]
- Hasselmo ME, Sarter M, 2011. Modes and models of forebrain cholinergic neuromodulation of cognition. *Neuropsychopharmacol* 36 (1), 52–73. 10.1038/npp.2010.104.
- Kanel P, van der Zee S, Sanchez-Catasus CA, et al. , 2022. Cerebral topography of vesicular cholinergic transporter changes in neurologically intact adults: a [18F] FEOBV PET study. *Aging Brain* 2, 100039. 10.1016/j.nbas.2022.100039. [PubMed: 35465252]
- Knott V, de la Salle S, Choueiry J, et al. , 2015. Neurocognitive effects of acute choline supplementation in low, medium and high performer healthy volunteers. *Pharmacol. Biochem. Behav* 131, 119–129. 10.1016/j.pbb.2015.02.004. [PubMed: 25681529]
- Kramer JH, Mungas D, Possin KL, et al. , 2014. NIH EXAMINER: conceptualization and development of an executive function battery. *J. Int. Neuropsychol. Soc JINS* 20 (1), 11–19. 10.1017/S1355617713001094. [PubMed: 24103232]
- Lim SAO, Kang UJ, McGehee DS, 2014. Striatal cholinergic interneuron regulation and circuit effects. *Front. Synaptic Neurosci* 6, 22. 10.3389/fnsyn.2014.00022. [PubMed: 25374536]
- Martinelli P, Sperduti M, Devauchelle AD, et al. , 2013. Age-related changes in the functional network underlying specific and general autobiographical memory retrieval: a pivotal role for the anterior cingulate cortex. *PLoS One* 8 (12), e82385. 10.1371/journal.pone.0082385. [PubMed: 24367516]
- McGeer PL, McGeer EG, Suzuki J, Dolman CE, Nagai T, 1984. Aging, Alzheimer's disease, and the cholinergic system of the basal forebrain. *Neurology* 34 (6), 741–745. 10.1212/wnl.34.6.741. [PubMed: 6539435]
- Mesulam MM, 2004. The cholinergic innervation of the human cerebral cortex. *Prog. Brain Res* 145, 67–78. 10.1016/S0079-6123(03)45004-8. [PubMed: 14650907]
- Mesulam MM, 2013. Cholinergic circuitry of the human nucleus basalis and its fate in Alzheimer's disease. *J. Comp. Neurol* 521 (18), 4124–4144. 10.1002/cne.23415. [PubMed: 23852922]
- Moreira NC. dos S., Lima JEB. de F., Marchiori MF, Carvalho I, Sakamoto-Hojo ET, 2022. Neuroprotective effects of cholinesterase inhibitors: current scenario in therapies for Alzheimer's disease and future perspectives. *J. Alzheimers Dis. Rep* 6 (1), 177–193. 10.3233/ADR-210061. [PubMed: 35591949]
- Natovich R, Gayus N, Azmon M, et al. , 2020. A comprehensive intervention for promoting successful aging amongst older people with diabetes with below-normal cognitive function—a feasibility study. *Front. Endocrinol* 11. 10.3389/fendo.2020.00348.
- Nejad-Davarani S, Koeppe RA, Albin RL, Frey KA, Müller MLTM, Bohnen NI, 2019. Quantification of brain cholinergic denervation in dementia with Lewy bodies using PET imaging with [18F]-FEOBV. *Mol. Psychiatr* 24 (3), 322–327. 10.1038/s41380-018-0130-5.
- Niemegeers P, Dumont GJH, Quisenbarts C, et al. , 2014. The effects of nicotine on cognition are dependent on baseline performance. *Eur. Neuropsychopharmacol* 24 (7), 1015–1023. 10.1016/j.euroneuro.2014.03.011. [PubMed: 24766971]
- Okkels N, Horsager J, Labrador-Espinosa MA, et al. , 2023. Distribution of cholinergic nerve terminals in the aged human brain measured with [18F]FEOBV PET and its correlation with histological data. *Neuroimage* 269, 119908. 10.1016/j.neuroimage.2023.119908. [PubMed: 36720436]
- Pardo JV, Nyabwari SM, Lee JT, 2020. Alzheimer's disease neuroimaging initiative. Aging-related hypometabolism in the anterior cingulate cortex of cognitively intact, amyloid-negative seniors at rest mediates the relationship between age and executive function but not memory. *Cereb Cortex Commun* 1 (1), tgaa020. 10.1093/texcom/tgaa020. [PubMed: 34296097]

- Parent M, Bedard MA, Aliaga A, et al. , 2012. PET imaging of cholinergic deficits in rats using [18F]fluoroethoxybenzovesamicol ([18F]FEOBV). *Neuroimage* 62 (1), 555–561. 10.1016/j.neuroimage.2012.04.032. [PubMed: 22555071]
- Petrou M, Frey KA, Kilbourn MR, et al. , 2014. In vivo imaging of human cholinergic nerve terminals with (–)-5-(18)F-fluoroethoxybenzovesamicol: biodistribution, dosimetry, and tracer kinetic analyses. *J. Nucl. Med. Off. Publ. Soc Nucl. Med* 55 (3), 396–404. 10.2967/jnumed.113.124792.
- Pezzoli S, Giorgio J, Martersteck A, Dobyns L, Harrison TM, Jagust WJ, 2024. Successful cognitive aging is associated with thicker anterior cingulate cortex and lower tau deposition compared to typical aging. *Alzheimers Dement J. Alzheimers Assoc* 20 (1), 341–355. 10.1002/alz.13438.
- Posner MI, Rothbart MK, 1998. Attention, self-regulation and consciousness. *Philos Trans. R Soc. B. Biol. Sci* 353 (1377), 1915–1927.
- Rockwood K, 2004. Size of the treatment effect on cognition of cholinesterase inhibition in Alzheimer's disease. *J. Neurol. Neurosurg. Psychiatry* 75 (5), 677–685. 10.1136/jnnp.2003.029074. [PubMed: 15090558]
- Rosa-Neto P, 2007. In: *Imaging Vesicular Acetylcholine Transporter in Rodents Using [18F] Fluoroethoxybenzovesamicol and Micro-PET*. Published online.
- Schliebs R, Arendt T, 2011. The cholinergic system in aging and neuronal degeneration. *Behav. Brain Res* 221 (2), 555–563. 10.1016/j.bbr.2010.11.058. [PubMed: 21145918]
- Schmitz TW, Nathan Spreng R, 2016. Basal forebrain degeneration precedes and predicts the cortical spread of Alzheimer's pathology. *Nat. Commun* 7 (1), 13249. 10.1038/ncomms13249. [PubMed: 27811848]
- Schmitz TW, Mur M, Aghourian M, Bedard MA, Spreng RN, 2018. Longitudinal Alzheimer's degeneration reflects the spatial topography of cholinergic basal forebrain projections. *Cell Rep.* 24 (1), 38–46. 10.1016/j.celrep.2018.06.001. [PubMed: 29972789]
- Sofroniew MV, Howe CL, Mobley WC, 2001. Nerve growth factor signaling, neuroprotection, and neural repair. *Annu. Rev. Neurosci* 24 (24), 1217–1281. 10.1146/annurev.neuro.24.1.1217. [PubMed: 11520933]
- Soucy JP, Rosa P, Massarweh G, et al. , 2010. P1-388: imaging of cholinergic terminals in the non-human primate brain using 18F-FEOBV PET: development of a tool to assess cholinergic losses in Alzheimer's disease. *Alzheimers Dement* 6 (4S\_Part\_10), S286. 10.1016/j.jalz.2010.05.942.
- Tan RH, Pok K, Wong S, Brooks D, Halliday GM, Kril JJ, 2013. The pathogenesis of cingulate atrophy in behavioral variant frontotemporal dementia and Alzheimer's disease. *Acta Neuropathol Commun.* 1, 30. 10.1186/2051-5960-1-30. [PubMed: 24252534]
- van der Zee S, Müller MLTM, Kanel P, van Laar T, Bohnen NI, 2021. Cholinergic denervation patterns across cognitive domains in Parkinson's disease. *Mov. Disord Off. J. Mov. Disord Soc* 36 (3), 642–650. 10.1002/mds.28360.
- Xia Y, Eeles E, Fripp J, et al. , 2022. Reduced cortical cholinergic innervation measured using [18F]-FEOBV PET imaging correlates with cognitive decline in mild cognitive impairment. *NeuroImage Clin.* 34, 102992. 10.1016/j.nicl.2022.102992. [PubMed: 35344804]

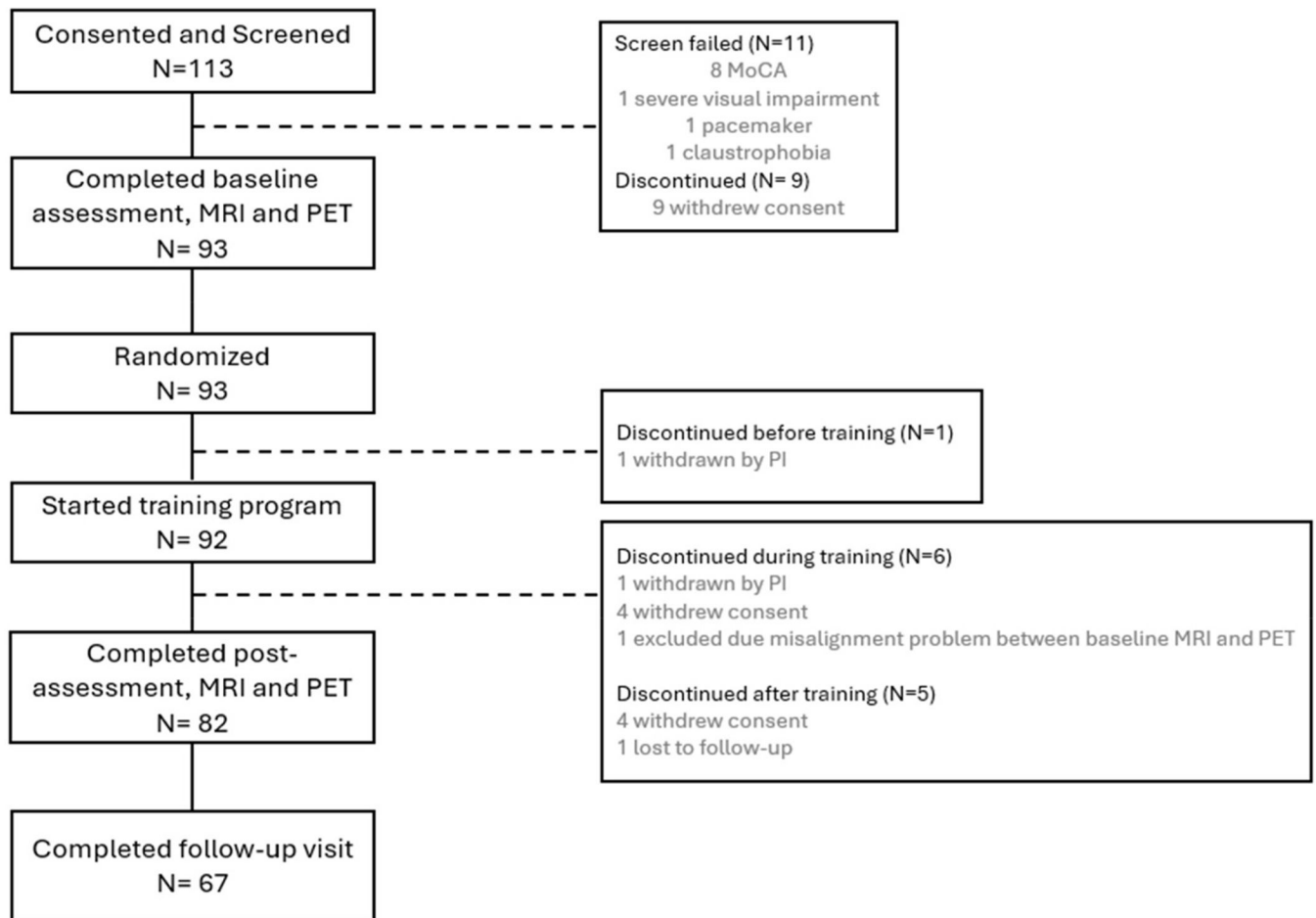


**Fig. 1.**  
Flowchart for the INHANCE trial. Abbreviations: PI, Principal Investigator; MoCA, Montreal Cognitive Assessment; MRI, Magnetic resonance imaging; PET, Positron emission tomography.



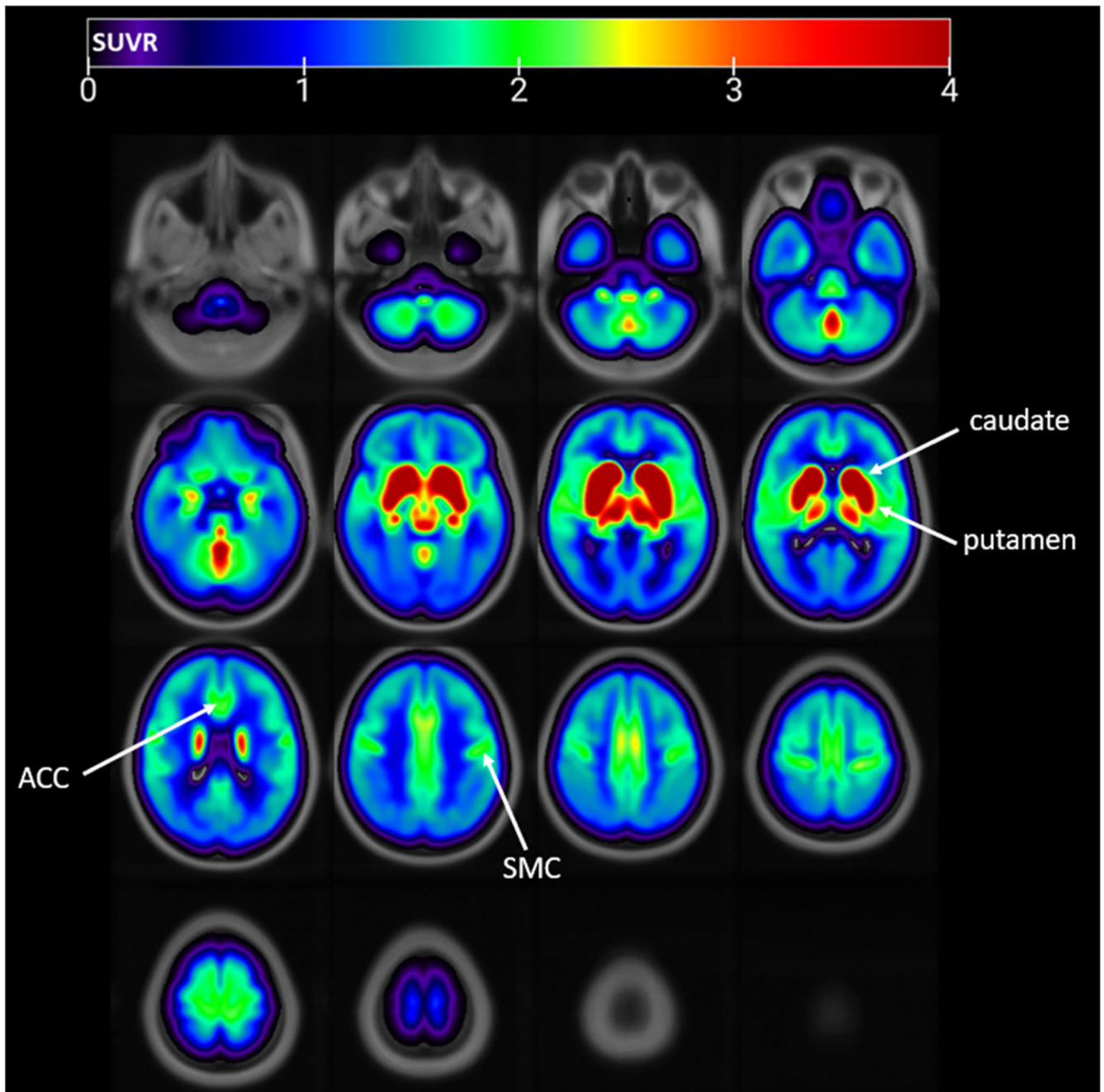


**Fig. 2.** FEOBV binding topography in averaged axial brain slices of the intent-to-treat population (N = 92). The [18F]FEOBV PET volumes are displayed in a mosaic of axial slices. Abbreviations: ACC, anterior cingulate cortex; SMC, primary sensorimotor cortex. Red colour indicates SUVR of 4 or higher.

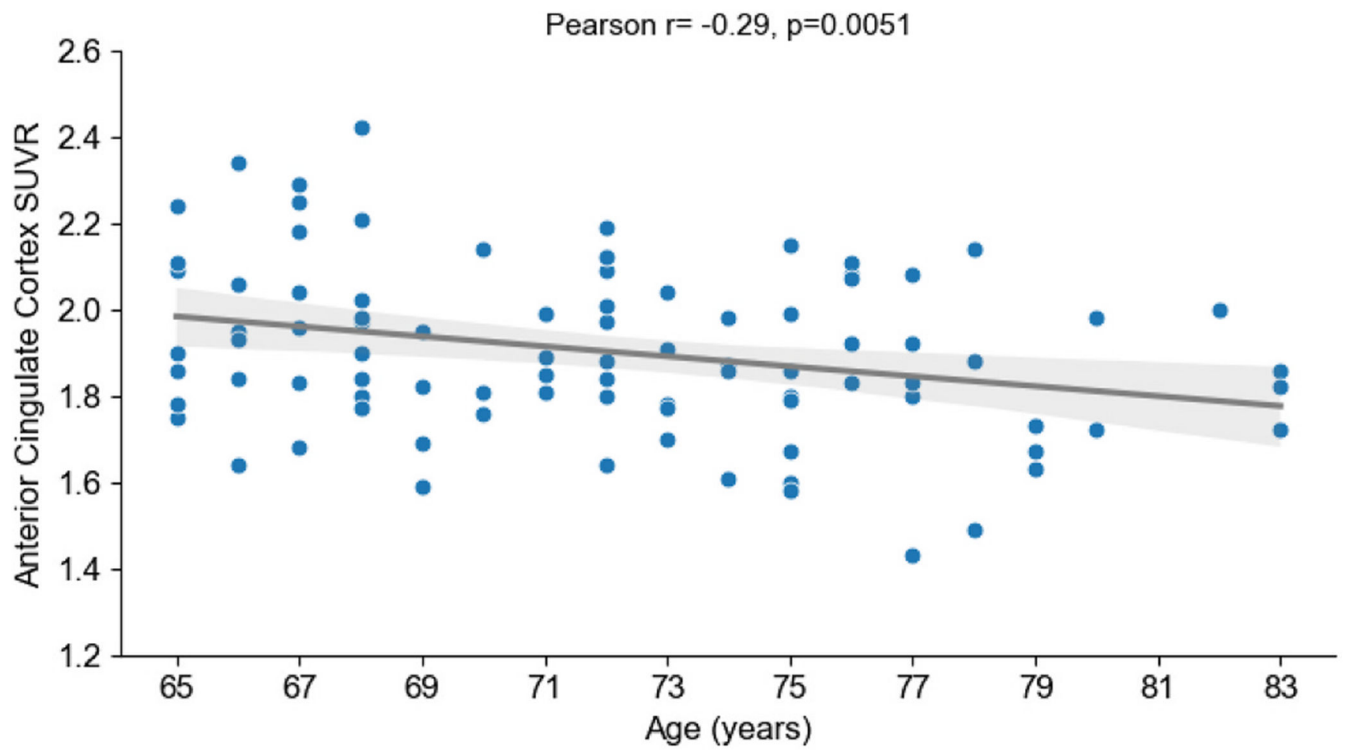


**Fig. 3.** Pearson correlation between baseline FEOBV binding in the anterior cingulate cortex and age for the intent-to-treat population ( $N = 92$ ). Each point represents an individual participant, with the regression line depicting the overall trend. Shaded regions around the regression lines represent 95% confidence intervals for the mean.

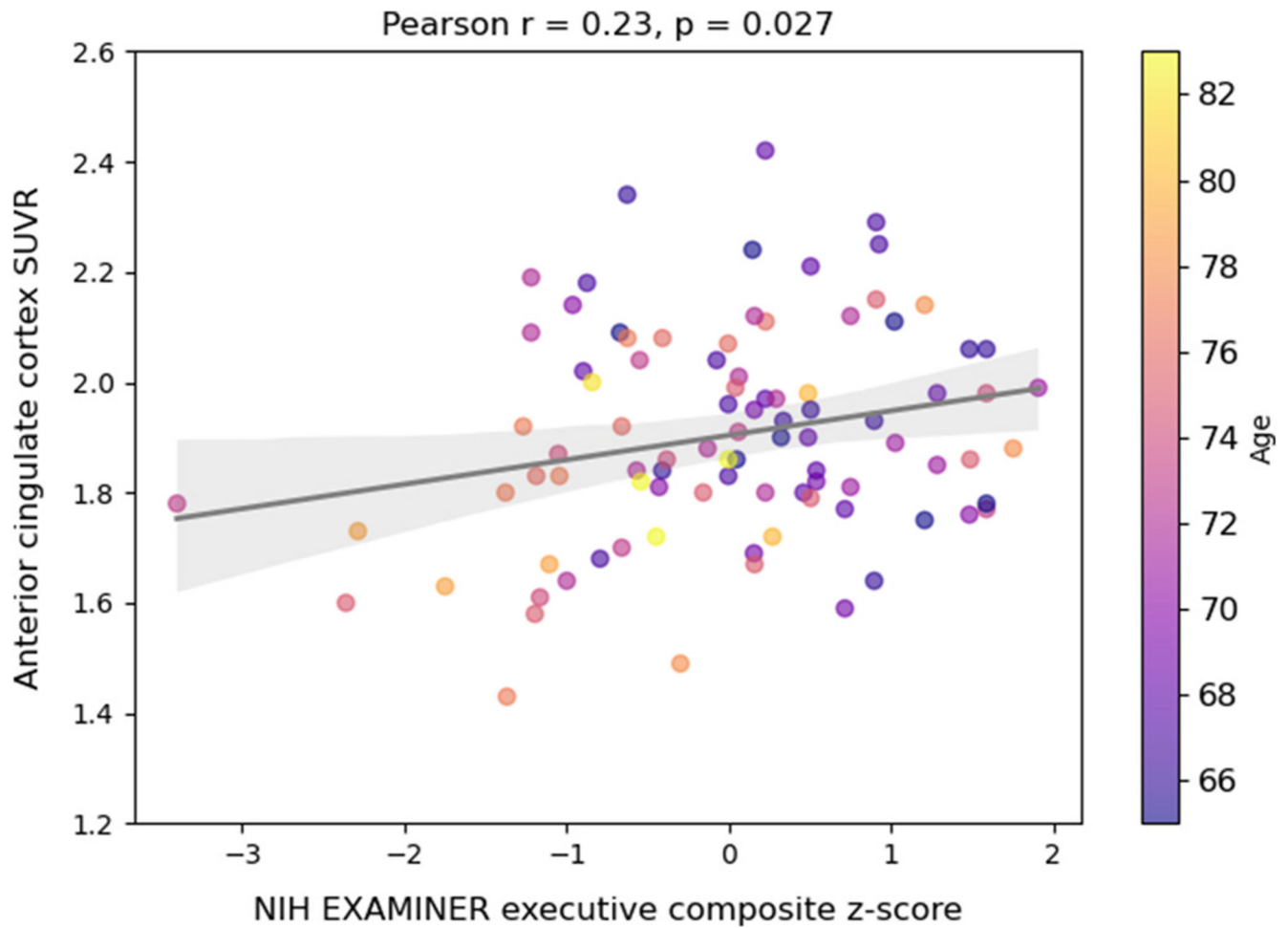


**Fig. 4.** Pearson correlation between FEOBV binding in the anterior cingulate cortex and the NIH EXAMINER executive composite z-score for the intent-to-treat population ( $N = 92$ ) with darker observation points representing participants of relatively younger age. Shaded regions around the regression lines represent 95% confidence intervals for the mean.

**Table 1**

Baseline characteristics of the intent-to-treat (ITT) population and all consented participants (N = 113).

| Participant's characteristics             | Intent-to-treat (ITT) (N = 92) | Consented (N = 113) |
|---|--------------------------------|---------------------|
| Age, mean (SD), years                     | 71.9 (4.9)                     | 71.9 (5.0)          |
| Education, mean (SD), years               | 16.5 (3.4)                     | 16.7 (3.4)          |
| Sex, n (%)                                |                                |                     |
| Female                                    | 61 (66)                        | 71 (63)             |
| Male                                      | 31 (34)                        | 42 (37)             |
| Race, n (%)                               |                                |                     |
| White                                     | 88 (96)                        | 106 (93)            |
| Asian                                     | 2 (2)                          | 4 (4)               |
| Black or African American                 | 1 (1)                          | 1 (1)               |
| American Indian/Alaska Native             | 0 (0)                          | 0 (0)               |
| Native Hawaiian or Other Pacific Islander | 0 (0)                          | 0 (0)               |
| More than one race                        | 0 (0)                          | 0 (0)               |
| Unknown or not reported                   | 1 (1)                          | 2 (2)               |
| Ethnicity, n (%)                          |                                |                     |
| Not Hispanic or Latino                    | 91 (99)                        | 110 (97)            |
| Hispanic or Latino                        | 0 (0)                          | 2 (2)               |
| Unknown or not reported                   | 1 (1)                          | 1 (0)               |
| Native Language, n (%)                    |                                |                     |
| English                                   | 33 (36)                        | 42 (37)             |
| French                                    | 50 (54)                        | 57 (50)             |
| Other Language                            | 9 (10)                         | 14 (13)             |
| Primary Language, n (%)                   |                                |                     |
| English                                   | 43 (47)                        | 55 (50)             |
| French                                    | 48 (52)                        | 57 (50)             |
| Other Language                            | 1 (1)                          | 1 (1)               |
| Bilingual, n (%)                          | 12 (13%)                       | 18 (16%)            |
| MoCA, total score (SD)                    | 26.2 (1.8)                     | Not applicable      |
| GDS-SF, total score (SD)                  | 1.4 (1.9)                      | Not applicable      |
| NIH EXAMINER, composite score (SD), raw   | 0.44 (0.57)                    | Not applicable      |

Abbreviations: ITT, intent-to-treat; SD, standard deviation; MoCA, Montreal Cognitive Assessment; GDS-SF, Geriatric Depression Scale - Short Form; NIH EXAMINER, National Institutes of Health The Executive Abilities: Measures and Instruments for Neurobehavioral Evaluation and Research.

Pearson correlations between FEOBV binding and age, NIH EXAMINER and MoCA across the pre-specified primary and exploratory ROIs for the ITT (N = 92) with bilaterally averaged FEOBV SUVRs and standard deviations (SD).

Table 2

| Region of Interest (ROI)    | Mean FEOBV SUVR (SD) | Correlations with Age |              | Correlations with NIH EXAMINER executive composite |             | Correlations with MoCA |      |
|-----------------------------|----------------------|-----------------------|--------------|--|-------------|------------------------|------|
|                             |                      | r                     | p            | r  | p           | r                      | p    |
| <b>Primary ROI</b>          |                      |                       |              |  |             |                        |      |
| Anterior cingulate cortex   | 1.90 (0.19)          | <b>-0.29</b>          | <b>0.005</b> | <b>0.23</b>  | <b>0.02</b> | 0.05                   | 0.62 |
| <i>Exploratory ROIs</i>     |                      |                       |              |  |             |                        |      |
| Posterior cingulate cortex  | 1.94 (0.20)          | <b>-0.20</b>          | <b>0.05</b>  | 0.13   | 0.22        | -0.09                  | 0.41 |
| Primary auditory cortex     | 2.01 (0.30)          | <b>-0.28</b>          | <b>0.008</b> | 0.13   | 0.23        | -0.02                  | 0.85 |
| Primary sensorimotor cortex | 1.73 (0.21)          | -0.12                 | 0.25         | 0.19   | 0.07        | -0.11                  | 0.30 |
| Global cortex               | 1.44 (0.14)          | -0.19                 | 0.07         | 0.16   | 0.13        | -0.12                  | 0.25 |
| Parietal lobe               | 1.46 (0.16)          | -0.17                 | 0.10         | 0.12   | 0.24        | -0.13                  | 0.21 |
| Frontal lobe                | 1.67 (0.17)          | -0.11                 | 0.29         | 0.07   | 0.48        | -0.10                  | 0.32 |
| Occipital lobe              | 1.20 (0.17)          | -0.19                 | 0.07         | 0.20   | 0.06        | -0.06                  | 0.60 |
| Temporal lobe               | 1.42 (0.17)          | -0.17                 | 0.10         | 0.14   | 0.17        | -0.12                  | 0.25 |
| Hippocampus                 | 2.13 (0.29)          | -0.13                 | 0.21         | 0.14   | 0.18        | -0.09                  | 0.37 |
| Parahippocampal gyrus       | 1.39 (0.21)          | -0.13                 | 0.21         | 0.12   | 0.23        | -0.09                  | 0.38 |
| Striatum                    | 6.09 (0.81)          | <b>-0.26</b>          | <b>0.01</b>  | 0.12   | 0.27        | 0.04                   | 0.69 |
| Putamen                     | 7.06 (0.98)          | <b>-0.27</b>          | <b>0.01</b>  | 0.11   | 0.28        | 0.04                   | 0.67 |
| Caudate                     | 5.11 (0.75)          | <b>-0.21</b>          | <b>0.05</b>  | 0.11   | 0.30        | 0.03                   | 0.75 |

Abbreviations: SUVR, standard uptake value ratios; MoCA, Montreal Cognitive Assessment.